

# **Sedimentary recycling in arc magmas; geochemical and U-Pb-Hf-O constraints on the Mesoproterozoic Suldal Arc, SW Norway**

Nick M W Roberts<sup>1,2</sup>, Trond Slagstad<sup>3</sup>, Randall R Parrish<sup>1,2</sup>, Michael J Norry<sup>1</sup>, Mogens Marker<sup>3</sup>, Matthew S A Horstwood<sup>2</sup>

<sup>1</sup>Department of Geology, University of Leicester, Leicester, LE1 7RH, UK.

<sup>2</sup>NERC Isotope Geosciences Laboratory, British Geological Survey, Nottingham, NG12 5GG, UK.

<sup>3</sup>Geological Survey of Norway, 7491 Trondheim, Norway.

## **Abstract**

The Hardangervidda-Rogaland Block within southwest Norway is host to ~1.52-1.48 Ga continental building, and variable reworking during the ~1.1-0.9 Ga Sveconorwegian orogeny. Due to the lack of geochronological and geochemical data, the timing and tectonic setting of early Mesoproterozoic magmatism has long been ambiguous. This paper presents zircon U-Pb-Hf-O isotope data combined with whole-rock geochemistry to address the age and petrogenesis of basement units within the Suldal region, located in the centre of the Hardangervidda-Rogaland Block. The basement comprises variably deformed grey gneisses and granitoids that petrologically and geochemically resemble mature volcanic arc lithologies. U-Pb ages confirm that magmatism occurred from ~1521 to 1485 Ma, and conspicuously lack any xenocrystic inheritance of distinctly older crust. Hafnium isotope data range from  $\epsilon\text{Hf}_{(\text{initial})}$  +1 to +11, suggesting a rather juvenile magmatic source, but with possible involvement of late Palaeoproterozoic crust. Oxygen isotope data range from mantle-like ( $\delta^{18}\text{O} \sim 5\text{‰}$ ) to elevated ( $\sim 10\text{‰}$ ) suggesting involvement of low-temperature altered material

(e.g. supracrustal rocks) in the magma source. The Hf-O isotope array is compatible with mixing between mantle-derived material with young low-temperature altered material (oceanic crust/sediments) and older low-temperature altered material (continent-derived sediments). This, combined with a lack of xenoliths and xenocrysts, exposed older crust, AFC trends and S-type geochemistry, all point to mixing within a deep-crustal magma-generation zone. A proposed model comprises accretion of altered oceanic crust and the overlying sediments to a pre-existing continental margin, underthrusting to the magma generation zone, and remobilisation during arc magmatism. The geodynamic setting for this arc magmatism is comparable to that seen in the Phanerozoic (e.g. the Sierra Nevada and Coast ranges batholiths), with compositions in the Suldal Sector reaching those of average upper continental crust. As within these younger examples, factors that drive magmatism towards the composition of the average continental crust include the addition of sedimentary material to magma source regions, and delamination of cumulate material. Underthrusting of sedimentary materials and their subsequent involvement in arc magmatism is perhaps a more widespread mechanism involved in continental growth than is currently recognized. Finally, the Suldal Arc magmatism represents a significant juvenile crustal addition to SW Fennoscandia.

## **Keywords**

Fennoscandia, zircon, arc magmatism, crustal recycling, Hf-O isotopes

## Introduction

The recycling of pre-existing continental crust, including sedimentary material, to arc magmas has long been recognised (e.g. Armstrong, 1971; Hildreth & Moorbath, 1988; Plank & Langmuir 1993). Numerous studies have sought to constrain whether continental crust has been recycled into the arc magmas in the mantle via subduction of sediments, or in the crust via assimilation and contamination (e.g. Hawkesworth et al., 1979; Thirlwall & Graham, 1984; Gasparon et al., 1994). Both of these processes probably occur together within the same volcanic arc system; but to determine rates and volumes of continental recycling, as well as crustal architecture, it is necessary to discriminate how and where crust is recycled. End-member processes comprise mantle recycling (i.e. source contamination) and intra-crustal recycling (i.e. crustal contamination); the latter can be broken down into infra-crustal recycling, whereby previously formed igneous crust (such as ancient underplated material) is recycled into the magma, and supracrustal recycling, whereby sedimentary material is recycled into the magma. Studies aiming at differentiating these processes have commonly combined radiogenic isotopes (e.g. Sr, Nd, Hf) with a stable isotope (i.e. O) (e.g. James, 1981; Davidson, 1985). More recently, studies have combined U-Pb, Hf and O isotopes measured within single zircon grains, and have demonstrated that both sedimentary and mantle material have been involved in the petrogenesis of a range of magma types in a variety of settings (e.g. I-type, Kemp et al., 2007; S-type, Appleby et al., 2009; A-type, Be'eri-Shlevin et al., 2009). Certain premises have been used in previous studies that recent research has shown to not be true, therefore adding further complexity to the understanding of petrogenetic processes from zircon Hf data. For example, subducted sediments that have a melt flux input to arc magmas will contribute to the Hf budget (e.g. Chauvel et al., 2009; Nebel et al., 2011), thus, both source and crustal contamination will affect the Hf signature of magmas; also, high melt and fluid flux from sediments and altered oceanic crust can lead to a contribution of  $\delta^{18}\text{O}$

(typically <2‰) from these sources into arc magmas (Bindeman et al., 2004; Martin et al., 2011); thus, also negating the use of  $\delta^{18}\text{O}$  as a clear discriminator of source versus crustal contamination.

The crystalline basement in SW Fennoscandia consists of various Palaeo- to Mesoproterozoic terranes (*sensu lato*) that comprise deformed plutonic and volcanic arc-like lithologies, that have been reworked during the Sveconorwegian (Grenvillian) and Caledonian orogenies (e.g. Gaál & Gorbatshev, 1987; Bingen et al., 2008a). The evolution of the ~1.7 to 1.5 Ga crust can be described by two end-member models: 1) Palaeoproterozoic crust underlies the entire region and has been recycled during younger magmatic episodes (Andersen et al., 2002b; 2004a; 2009b), or 2) the various terranes represent accreted juvenile arcs with limited contribution from older material (Brewer et al., 1998; Åhäll & Connelly, 2008). Various isotope data point to a contribution from Palaeoproterozoic crust to both Gothian aged (~1.7-1.55 Ga) and Sveconorwegian magmatism (1.2-0.93 Ga; Andersen, 1997; Andersen et al., 2001; 2002b; 2004a; 2007b; 2009b; Andersen & Griffin 2004; Pedersen et al., 2009). In the Hardangervidda-Rogaland and Telemark Blocks, ~1.5 Ga units are widespread and are the oldest exposed crust currently dated (Bingen et al., 2005; 2008b; Pedersen et al., 2009), but are hitherto poorly understood. The present study combines whole-rock geochemical and zircon U-Pb, Hf and O data from Telemarkian-aged (~1.52-1.48 Ga; Bingen et al., 2008a) rocks in the Suldal region of southwest Norway (Fig. 1); the data are used to constrain the tectonic setting and petrogenesis of associated magmatism, and constrain the role that recycling of pre-existing crust has had in the formation of Telemarkian crust; this Proterozoic example of arc magmatism is compared to the Phanerozoic western US Cordillera, with similarities suggesting similar processes of continental crust formation existing since the mid-Proterozoic.

## **Geological Setting**

The Fennoscandian Shield comprises an Archaean core in the northwest; surrounding this are younger arcs and microcontinents that amalgamated during the Svecofennian orogeny at ~ 2.1-1.9 Ga (Korja et al., 2006; Lahtinen et al., 2009). At ~1.85 Ga, a subduction zone initiated on the southwest margin (present-day position) of the continent, producing the Transcandinavian Igneous Belt (TIB; see Högdahl et al., 2004). The terranes to the southwest of the TIB that comprise the Southwest Scandinavian Domain (SSD), can be interpreted as forming in continental and island arcs along a long-lived subduction margin that progressively moved away from the Fennoscandian continent (Åhäll & Connelly, 2008) in a retreating accretionary orogen (Cawood et al., 2009).

The SSD comprises crustal blocks (variably referred to as terranes and domains in the literature) aged ~1.69 to 1.48 Ga that progressively young to the west; here we conform to the nomenclature outlined in Andersen (2005). The Hardangervidda-Rogaland (HRB) and Telemark Blocks (TB) comprise the majority of crust west of the Oslo Rift (Andersen, 2005), and correlate to the Telemarkia terrane of Bingen et al. (2005, 2008a). So far, the oldest identified igneous unit within these blocks is the 1.55 Ga Åsen metatonalite (Pedersen et al., 2009); this is the only unit older than 1.52 Ga, and its origin remains uncertain. The main continental growth episode within the HRB-TB is defined as 1.52-1.48 Ga (Bingen et al., 2005b; 2008a), and is known from dating plutonic and volcanic orthogneisses from across the region. Other major tectonostratigraphic units within the HRB-TB include the volcano-sedimentary ~1.5-1.35 Ga 'Vestfjorddalen' Supergroup (terminology of Laajoki et al., 2002). This has been suggested to be a continental rift basin that started forming at ~1.51 Ga, and by ~1.35 Ga had extended into an epicontinental sea (Lamminen & Köykä, 2010); associated

with extension was voluminous felsic volcanism (Tuddall Fm.) followed by voluminous basic magmatism (Vemork Fm.), with a suggested tectonic setting inboard of a subduction zone in a setting similar to the Granite-Rhyolite provinces in the mid-continental US (Slagstad et al., 2009). Other supracrustal sequences dated at 1260-1220 and 1170–1140 Ma are found across the HRB-TB, and are also related to extensional settings possibly inboard of a subduction margin (Bingen et al., 2002; Brewer et al., 2004; Roberts et al. 2011). Early- to late-tectonic Sveconorwegian granitoids intrude the region and are dated between 1.05 and 0.93 Ga (Andersen et al., 2002a, 2007a; Bingen & van Breemen, 1998; Schärer et al., 1996; Slagstad et al., 2012; Vander Auwera et al., 2011).

The origin of the HRB and TB (i.e. Telemarkia terrane of Bingen et al., 2005) is under debate, it may resemble an exotic crustal fragment accreted during the Sveconorwegian orogeny, a crustal fragment that originated further north along the Fennoscandian margin, or an indigenous part of the SW Fennoscandian crust (see Andersen, 2005 and Bingen et al., 2005 for discussion). Various sedimentary units that were deposited on these blocks between ~1.6 and 1.1 Ga, contain Palaeoproterozoic and late Archaean detrital zircons (Åhäll et al., 1998; de Haas et al., 1999; Bingen et al., 2001, 2003; Andersen et al., 2004b); this suggests that during the Mesoproterozoic these blocks were located near to an older continental craton. Detrital zircons from the 'Vestfjorddalen' Supergroup feature a major peak at 1730 Ma and a lack of peaks between 1650-1500 Ma; this contrasts with the age of the Fennoscandian basement and is suggested to reflect an original location of the Telemark Block closer to the Laurentian craton rather than Fennoscandia (Lamminen & Köykkä, 2010). Whole-rock isotope and in-situ zircon isotope studies on Sveconorwegian magmatism indicate addition of an older crustal component that has a model age of >1.7 Ga, and a mantle component that is 1.2 Ga and/or younger (Andersen et al., 2001; 2002b; 2007b; 2009b; Andersen & Griffin,

2004; Pedersen et al., 2009). These data were used to suggest a 1.7-1.9 Ga TIB-like lower crust that extends under the whole of southern Norway (Andersen et al., 2009b), and also to imply an indigenous rather than exotic origin for the Telemark Block (Andersen et al., 2002b; 2004a; Pedersen et al., 2009).

## **Geology of the studied gneiss/granitoid complex**

Studied samples are from the Sauda and Suldal communes (Figure 1). The original mapping of the Sauda region by Sigmond (1975, 1978) defined three separate supracrustal belts and an inferred older gneiss complex. Recent mapping reveals that fine-grained lithologies probably representing supracrustal units are found throughout the region, and are inter-mingled with hypabyssal and coarse-grained plutonic lithologies. The petrology and field-relations are interpreted as representing the deformed mid- to supracrustal remnant of a volcanic arc terrane. The grey gneisses (*sensu lato*) that dominate exposures in the Sauda-Suldal region are here named the Sauda Grey Gneiss Association (SGGA).

### **The Sauda Grey Gneiss Association**

The SGGA is a heterogeneous complex of orthogneisses, comprising gabbro, diorite, granodiorite, granite and tonalite compositions, along with minor syenite. All lithologies are metamorphosed to amphibolite-facies with variable regression in greenschist-facies; however, the meta-prefix is omitted here for simplicity. The complex is dominated by fine to medium-grained porphyritic grey gneisses. Some outcrops feature banding, commonly between aphyric and phyrlic units, likely representing volcanic tuff/ignimbrite/lava (i.e. supracrustal) layers. Medium-grained porphyritic gneisses likely represent hypabyssal/upper crustal intrusions. Within the Sauda-Suldal region, units with obvious paragneiss affinities were not observed. Magmatic enclaves are common within the SGGA, and are of variable lithologies.

The most common are fine-grained mafic to felsic xenoliths within granodioritic gneisses, but also displayed are tonalitic/granitic enclaves in more mafic units, often interpretable as disaggregated veins/dykes. Some outcrops include evidence of magma mingling, the best example of this comprises aphyric granodioritic gneiss mingling with aphyric dioritic gneiss; margins between the two lithologies are rounded suggesting contemporaneous intrusion. Partial melting within the Grey Gneiss is evident in some outcrops, usually without large-scale separation of leucosome and melanosome; however, in a few exposures leucosomes of tonalitic material have formed a network of cm-scale veins which are normally sub-parallel to the structural fabric. A few outcrops of fine-grained banded gneiss exhibit patch-leucosome formation, with new growth of hornblende within the leucosomes.

### **Granitoids**

Weak to moderately deformed coarse-grained porphyritic granodiorites occur as sheets within the Grey Gneiss complex, ranging from metres to tens of metres in width. These are conformable to the fabric of the Grey Gneiss, and have a range of sharp to graded contacts into the Grey Gneiss lithologies. Undeformed bodies of porphyritic granite also occur; these have varying mafic content, grading from porphyritic biotite-hornblende granodiorites to porphyritic biotite granites, and probably represent zoned plutonic bodies. The distinction between ~1500 Ma plutonic bodies and those of Sveconorwegian (~1.05-0.95 Ga) age is unclear, as both deformed and undeformed examples of each exist; however, the latter often have reddish feldspar phenocrysts compared to the white-grey feldspar phenocrysts in the former.

### **Timing of magmatism**

Previous age determinations have been made using a variety of methods, on thirteen meta-volcanic and plutonic lithologies within the Sauda-Suldal region by Bingen et al. (2005); the zircon crystallization ages ranged from  $1491 \pm 5$  to  $1519 \pm 12$  Ma. New zircon ages were determined within this study on twelve different lithologies (see supplementary online material; figure 2), with ages ranging from  $1485 \pm 11$  to  $1521 \pm 6$  Ma.

## **Zircon textures**

Separated zircons from the samples of this study have a range of morphologies, but are generally prismatic, oscillatory-zoned and elongate, as is typical of igneous zircons (e.g. Corfu et al., 2003). The more mafic lithologies (SA7-86 and ROG525) exhibit larger zircons which were fragmented during separation, and feature less distinct oscillatory-zoning or are sector zoned (see supplementary online material). Distinctive core and rim/overgrowth relationships are lacking in all samples. Discontinuities in zoning exist in some grains, but the style of zoning across these is similar, suggesting an origin related to replenishment of magma during crystallisation, as opposed to overgrowth on inherited zircons.

## **Geochemistry**

### **Sauda Grey Gneiss Association**

The samples range from gabbro and diorite, through tonalite and granodiorite/dacite to granite/rhyolite. The geochemistry of the SGGA is calcic to calc-alkaline, metaluminous to weakly peraluminous, and displays a magnesian trend typical of Cordilleran arc magmas (see Figure 3). In Harker diagrams the SGGA displays broadly negative trends for  $\text{Al}_2\text{O}_3$ ,  $\text{TiO}_2$ ,  $\text{CaO}$ ,  $\text{MgO}$ ,  $\text{MnO}$ ,  $\text{Fe}_2\text{O}$  and  $\text{P}_2\text{O}_5$ , and broadly positive trends for  $\text{Na}_2\text{O}$  and  $\text{K}_2\text{O}$ . Trends for Large Ion Lithophile elements (LILE) are scattered, but positive for Rb and Ba, and negative

for Sr after ~65% SiO<sub>2</sub>. The transition metals (e.g. V; Figure 3) show negative trends. High Field Strength Elements (HFSE), e.g. Nb and Zr, show slightly positive trends but with considerable scatter. All Rare Earth Elements (REEs) show scattered positive trends, with considerably less scatter at <66-70% SiO<sub>2</sub>.

In Primitive Mantle-normalised multi-element diagrams (Figure 4), all lithologies show enrichment in all elements relative to Primitive Mantle; the greatest enrichment is that of the LILE, and strong depletion relative to other elements is seen in Nb, Ta, Sr, P and Ti. In chondrite-normalised REE diagrams (Figure 4), all lithologies show LREE enrichment relative to MREE, LREE enrichment relative to HREE, and only slight MREE enrichment relative to HREE. In basaltic samples both small negative and positive Eu anomalies are exhibited; with increasing silica enrichment the Eu anomaly becomes progressively more negative.

### **Granitoids**

The granitoids are porphyritic, granodioritic to granitic, calc-alkaline and metaluminous to weakly peraluminous (Figure 3). The majority of the samples plot in the ferroan field (Fe\*; Figure 3); however, this does not definitively mean they have evolved from less-differentiated ferroan magmas, since at high silica content most magmas become enriched in Fe\* (Frost et al., 2001). The granitoids have similar major and trace element contents to those in the SGGA. In Primitive Mantle-normalized multi-element diagrams (Figure 4) the granitoids display similar enrichment and depletions to those of the most evolved members of the SGGA.

### **Petrogenesis**

The LILE enrichment and depletion in Nb, Ta, P and Ti are all characteristic of magmas produced in a supra-subduction zone setting. The HFSE enrichment in the SGGA is typical of continental arc magmas. This enrichment, which is not typically observed in intra-oceanic arcs, is often related to an enriched source, e.g. asthenospheric mantle as opposed to depleted mantle, and/or to crustal contamination (i.e. the 'within-plate' component; Pearce, 1983). The large range from mafic to felsic compositions indicates that partial melting of pre-existing felsic crust did not form the SGGA, as the compositions would then be dominantly granitic. The differentiation trends, with various inflections in many elements, suggest fractional crystallisation played a significant role in magmatic differentiation of the SGGA and granitoids. The trends displayed are typical of POAM - Plagioclase, olivine (and/or orthopyroxene), clinopyroxene (and/or amphibole) and magnetite fractionation; such fractionation is typical in arc suites for the formation of andesitic compositions from mafic parent melts (Gill, 1981). According to the REE modeling of Brophy (2008), the slightly increasing LREE and constant HREE at intermediate compositions are compatible with amphibole-present basalt fractionation in the lower crust, and the enrichment in all REE at high silica content is compatible with mid-to upper-crustal fractionation of basalt where amphibole is not present.

The geochemistry of the SGGA (and associated granitoids) indicates formation by fractional crystallisation of a basaltic parent melt, with multiple stages of fractionation occurring at different levels within the crust; partial melting of already crystallised lithologies would also have driven the upper crust to more felsic compositions. This scenario is compatible with a deep hot crustal zone setting (Annen et al., 2006). The geochemistry of the studied suites suggests formation in a volcanic arc, with the enrichment in HFSE, and range and abundance of evolved compositions being indicative of a mature island arc or continental arc (i.e. thick

crustal pile). The term Suldal Arc is hereby used to refer to this volcanic arc setting at ~1500 Ma.

### **Hf isotopes in zircon**

Hafnium isotopes were measured in eleven samples from the SGGA and associated granitoids (see figure 5). Each sample has a mean value falling between CHUR and depleted mantle (DM); the total  $\epsilon\text{Hf}$  range across the samples is from  $\sim+1$  to  $+11$ . The range in  $\epsilon\text{Hf}$  for each sample varies from  $\sim 1.5$  to 6 epsilon units (MSWD 0.4 to 5), which is within analytical uncertainty for some samples (MM36631, MM36676, SA3-60, SA7-91; MSWD 0.4 to 1.4). Twenty of the analyses lack corresponding U-Pb data from the same zircon; however, the U-Pb data from these samples suggest the zircons represent single igneous populations (see supplementary files), and therefore the intrusion age provides a robust estimate for the age of crystallisation of the zircons. The lack of anomalously low  $^{176}\text{Hf}/^{177}\text{Hf}_{\text{initial}}$  in any of the samples suggests that none of the analyses were conducted on grains inherited from much older crust (e.g.  $>300$  Myrs). Multiple Hf isotope analyses from the same zircon grain are within analytical uncertainty of each other, with the maximum variation within a single grain being no more than  $\sim 2$  epsilon units; this indicates there may have been a lack of evolving heterogeneity in the host magmas, in contrast to some previous studies (Kemp et al., 2007; Appleby et al., 2008; Be'eri Shlevin et al., 2009). The data exhibit a subtle temporal correlation, with  $\epsilon\text{Hf}$  decreasing through time (Figure 5); however, it should be noted that many of the ages have overlapping uncertainties, and the trend is not compelling.. The data do not exhibit a correlation between  $\epsilon\text{Hf}$  and  $\text{SiO}_2$  (i.e. magma differentiation); intermediate lithologies exhibit the most evolved Hf signatures.

### **Oxygen isotopes in zircon**

A subset of eight samples were analysed for  $\delta^{18}\text{O}$  (Figure 6). The average  $\delta^{18}\text{O}$  of each sample varies from  $+5.4 \pm 0.9$  to  $+8.7 \pm 1.2$  ‰. Five of the samples have variation which does not exceed analytical uncertainty (ROG525, SA3-04, SA3-60, SA7-86, SA7-91; MSWD = 0.7 to 1.7), and two of the samples have slightly larger variation suggesting the host magma had a degree of heterogeneity (MM2235, MM2241; MSWD = 2.8 & 3.3). One sample (SA7-04) exhibits a significant range in  $\delta^{18}\text{O}$  (~4 ‰); zircons from this sample have been affected by lead-loss, has metamict and/or alteration textures visible in CL, and under normal light the zircons exhibit an opaque milky colour (see supplementary files). The sample was taken from near a contact to a Sveconorwegian intrusion which features hydrothermal mineralization; thus, it is suggested that the variation in  $\delta^{18}\text{O}$  within this sample may represent post-crystallisation alteration. Where multiple  $\delta^{18}\text{O}$  ratios have been measured on the same zircon grain, there is variation of up to 1.0 ‰, which is slightly outside of analytical uncertainty ( $\pm 0.7$  ‰); these multiple analyses were not conducted on distinguishable growth zones, as such analyses were hampered by the limited availability of material to analyse. The oxygen isotope data do not exhibit a clear correlation with  $\text{SiO}_2$ , nor do they exhibit a defined trend with age.

## **Discussion**

### **Isotopic constraints on magma source**

The exposed basement in the Sauda-Suldal region is interpreted as representing a deformed mature volcanic arc (i.e. the Suldal Arc), with U-Pb ages indicating a lifespan from at least ~1521 to 1485 Ma. The following section will discuss new and published isotopic data that shed light on the nature of the magma source to the Suldal Arc and associated ~1.5 Ga magmatism within the Hardangervidda-Rogaland and Telemark Blocks..

The range in  $\epsilon\text{Hf}_{(T)}$  from +1.1 to +11.3 is suggestive of involvement of older crust to the Suldal Arc magmatism, with model ages pointing to late Palaeoproterozoic crust (Figure 7). This is in accord with Andersen et al. (2002b; 2004b; 2009b) who postulate a deep crustal reservoir beneath the whole of southern Norway that is 1.7-1.9 Ga in age. The range in  $\epsilon\text{Hf}_{(T)}$  is slightly more evolved than in arc lithologies (granodiorite/tonalite) sampled from the Bamble-Lillesand and Kongsberg-Marstrand Blocks terranes to the east of the HRB (Figure 7), suggesting either: 1) a greater input of a similar crustal component to the Suldal Arc magmatism, or 2) a change in the crustal component across strike.

In Precambrian studies, evolved  $\epsilon\text{Hf}_{(T)}$  is sometimes inferred to represent older crust being located at depth, i.e. intracrustal recycling (e.g. Bickford et al., 2008; Andersen et al. 2009b); however, in some modern arcs a deviation from depleted mantle in  $\epsilon\text{Hf}_{(T)}$ , has been correlated to contamination within the mantle from subducted oceanic crust and the overlying terrigenous sediments, i.e. mantle recycling (e.g. Chauvel et al., 2009; Tollstrup et al., 2010; Nebel et al., 2011). Thus, although Hf isotopes can fingerprint crustal contamination within arc magmas, they alone do not allow the pathways of recycling to be determined, and thus also do not constrain unexposed crustal architecture. Deducing the pathways of contamination in arc magmas has been a long-standing topic (e.g. Hawkesworth et al., 1979; Thirlwall & Graham, 1984), such contamination pathways are distinguished as (1) source contamination, whereby subducted sediments impart a signature on the mantle and lead to an influence on the associated arc magmatism; and (2) crustal contamination, whereby mantle-derived magmas are influenced by the crust that they intrude, via assimilation and wall-rock interaction. In modern arcs, the combination of stable (i.e. oxygen) with radiogenic (i.e. Nd, Sr, Hf) isotopes has been used widely to discriminate contamination processes; in recent years, this has been applied to older arc magmas where whole-rock oxygen isotopes would be rendered unreliable

due to alteration, by using in-situ zircon isotope analyses. The benefit of single mineral isotopes is that averaging of different sources in bulk whole-rock measurements is avoided, allowing for heterogeneous sources to be better fingerprinted (e.g. Peck et al., 2004; Lackey et al., 2005; Bolhar et al., 2006; Kemp et al., 2007).

The traditional premise behind the use of oxygen isotopes is that the mantle is assumed to be a remarkably homogeneous oxygen isotope reservoir, with igneous zircons formed in equilibrium with the mantle having an average  $\delta^{18}\text{O}$  of  $5.3 \pm 0.3 \text{ ‰}$  (Valley et al., 1998). High magmatic  $\delta^{18}\text{O}$  values ( $>6.5\text{‰}$ ) are attributed to melting or assimilation of sediments, altered volcanics, or other supracrustal rocks affected by low-temperature alteration, whereas low magmatic  $\delta^{18}\text{O}$  values ( $<5\text{‰}$ ) are attributed to incorporation of material that has undergone high temperature alteration, e.g. lower oceanic crust (Valley et al., 2005). Oxygen isotopes have therefore been used to discriminate source contamination (mantle recycling) from crustal contamination (intracrustal recycling) (e.g. James, 1981; Davidson, 1985), using the premise that source contamination will lead to enriched radiogenic isotope signatures, but with oxygen isotopes retaining a mantle signature. The assumption of a homogeneous mantle reservoir has been hampered by recent research that has shown the existence of heterogeneity in mantle oxygen isotope signatures, this has been related to fluxing of high  $\delta^{18}\text{O}$  melt and/or fluids into the mantle from sediments and the upper part of the downgoing oceanic slab within subduction zones (Eiler et al., 2005; Portnyagin et al., 2007; Auer et al., 2009; Johnson et al. 2009; Martin et al. 2011); these studies have shown up to  $\sim 2 \text{ ‰}$  elevation above the mantle range in mafic melts, although most are typically  $<1 \text{ ‰}$ .

The spread of data within Hf-O isotope space can be used to help determine pathways under which different isotopic reservoirs have combined. Given that oxygen concentrations in

sediments, crust and mantle are broadly similar, the shape of mixing/assimilation curves within Hf-O space is largely controlled by the Hf concentrations of the various components. The Suldal Arc data that comprise Hf and O isotopes measured within the same zircon, are plotted in Figure 8; the data form a broad array that can be loosely interpreted as mixing between two or more components, i.e. a mantle-like component and an older (low  $\epsilon\text{Hf}$ ) 'crustal' component that has been altered at low-temperature (high  $\delta^{18}\text{O}$ ). In previous studies on much younger magmatism, crustal/sedimentary end-members can be sampled directly (e.g. Vroon et al., 2001; Kemp et al., 2007; Nebel et al., 2011), allowing a greater confidence in mixing/assimilation calculations. In the present study there are no metasediments, xenoliths or exposed older crust within the region of the studied magmatism, thus, any crustal end-members have to be estimated, and mixing/assimilation models remain speculative; however, they provide pertinent information regarding the overall processes of crustal recycling. The crustal end-member modeled in figure 8 corresponds to the average  $\epsilon\text{Hf}$  of metasediments exposed in the adjacent and slightly older Kongsberg-Marstand Block (see figure 1), which have deposition ages of  $\sim 1.5$  Ga and slightly older. These supracrustal rocks are a proxy for high  $\delta^{18}\text{O}$  sediments that may have been subducted beneath the Suldal Arc, or were deposited in surrounding basins and on any pre-existing crust. The crustal end-member also overlaps in  $\epsilon\text{Hf}$  composition with the 1.7-1.9 Ga Transscandinavian Igneous Belt (TIB) that is exposed further east within Sweden, and is a proxy for the 1.7-1.9 Ga deep crustal reservoir underlying southern Norway hypothesised by Andersen et al. (2002b; 2009b). Figure 8a shows bulk-mixing curves for mixing between depleted mantle and the crustal end-member with both upper- and lower-crustal Hf concentrations (5.3 and 1.9 ppm Hf respectively); in these cases the mixing curves fall below the majority of the data. The rather straight array exhibited by the data, instead suggests mixing between components that have similar Hf concentrations (i.e. enriched crust/mantle rather than depleted mantle), and the elevated  $\delta^{18}\text{O}$  of primitive

compositions suggest introduction of a high  $\delta^{18}\text{O}$  component early on in magma differentiation, i.e. to the magma source region. To demonstrate this, figure 8b shows two mixing curves between a component that approximates old crust/sediments with high  $\delta^{18}\text{O}$ , and a component that approximates a mixed mantle/crustal source with moderately elevated  $\delta^{18}\text{O}$ . The latter component may comprise young altered sediments and/or oceanic crust, as well as depleted mantle that has been enriched by a high  $\delta^{18}\text{O}$  source; the data do not constrain the degree that each of these may have influenced the magmas. In summary, the Hf-O data indicate a mixture of enriched mantle, and low-temperature altered young and old components.

#### **Constraining contamination pathways**

Mixing and assimilation in magmas can occur at a variety of levels within a magmatic plumbing system; to determine where this has occurred in the Suldal Arc, a variety of evidence is examined. Upper crustal contamination (i.e. late-stage magmatic contamination) typically leaves xenoliths and/or xenocrysts of the host rock within intruding magmas. Within the Suldal Arc, xenoliths of sedimentary origin are absent; instead, xenoliths are of igneous origin and can be thought of as enclaves, thus, they are interpreted as evidence of magma mingling within the arc. Arc magmas that have assimilated older felsic crust/sediments typically contain inherited zircons that exhibit older U-Pb ages; although, the survival of inherited zircons is variable, and depends on factors including zircon size, magma temperature and magma chemistry (e.g. Watson & Harrison, 1983; Watson, 1996; Miller et al., 2003). There is no evidence of inheritance of distinctly older crust within the Suldal Arc (see figure 2). It could be argued that the Suldal Arc magmas have dissolved all xenocrystic zircons; however, there is a range in chemistry and crystallisation temperatures of the magmas

sampled (zircon saturation temperature ranges from 717 to 861°C; see supplementary files), which would likely lead to zircons surviving in at least some of the lithologies.

Assimilation in the upper crust (i.e. late-stage contamination) leads to trends that involve contamination indices increasing with those of magma differentiation (e.g. SiO<sub>2</sub>). In the Suldal Arc the Hf and O isotope data do not reveal traditional Assimilation Fractional Crystallisation (AFC) trends (figures 5 & 6), suggesting but not confirming that AFC did not control isotopic variations. Assimilation of altered material (i.e. high δ<sup>18</sup>O) such as sediments, will typically impart a signature on the whole-rock geochemistry of magmas; this has led to the S-type classification of granites that have involved sediments in their source (Chappell & White, 1974). The whole-rock geochemistry of the Suldal Arc lacks any S-type traits (e.g. elevated Al<sub>2</sub>O<sub>3</sub> and low Na<sub>2</sub>O), suggesting igneous rather than sedimentary sources were dominant. It should be noted that previous studies have revealed sedimentary input to magma sources with no clear indication within the whole-rock geochemistry of granites (Kemp et al., 2007).

All of the evidence points to a deep-crustal input of the high δ<sup>18</sup>O components into the magma-generation zone. Through a deep-crustal mixing process, any sedimentary geochemical signature will be diluted with a mantle-derived geochemical signature. Also, a deep mixing zone means that zircons from any older felsic components are more likely to have been dissolved within the melts because this region will be hotter relative to the upper crust. From the mixing trends shown, the degree of contamination is high (>30%), requiring very high temperatures; thus, energy conservation constraints also point to a hot and thus deep crustal melting region. This leaves the remaining major question: how do low-temperature

young and old components have a large degree of input into a deep-crustal magma-generation zone?

### **Sedimentary recycling in arc magmas**

The emplacement of sedimentary material into the source region of an arc can occur through:

1) subduction of sediments that lie upon the descending slab (and subsequent slab and sediment fluid-fluxing and/or slab melting), 2) underthrusting, underplating and/or relamination (Hacker et al., 2011) of sedimentary material to the base of the over-riding crust, or 3) by tectonic burial of sedimentary material that was deposited upon the over-riding crust.

The latter process is difficult to envisage for the Suldal Arc, since some evidence of a former complex crustal architecture where sediments have been interleaved and buried within pre-existing continental crust is expected to be preserved. Such a process can account for formation of granites within the Lachlan fold belt in SE Australia, where exposure of metasedimentary country rocks is abundant, and granites with high- $\delta^{18}\text{O}$  are seen to intrude the country rock (Kemp et al., 2007; 2009). The first process is considered unlikely to be the sole cause, since this deeply subducted source should lead to much smaller degrees of contamination, and as yet has not been evidenced to produce such elevated oxygen signatures as seen in this example. The second process, i.e. underthrusting and underplating, is invoked in more modern continental arc settings, i.e. the Sierra Nevada & Coast Mountain Batholiths (Lackey et al., 2005; Wetmore & Ducea, 2011); in these examples, high- $\delta^{18}\text{O}$  sediments and altered oceanic crust/plateau are subducted and underthrust during preceding arc magmatism, particularly during periods of enhanced subduction erosion, and are then remobilised during formation of the batholith. The underthrusting/underplating of continental material 'preconditions' the lithospheric mantle region (Lackey et al., 2005), i.e. gives it an elevated oxygen signature. Such a scenario will lead to the following record: 1) relatively primitive

radiogenic isotope signatures indicating a young contaminant, 2) I-type geochemistry suggesting a mafic to intermediate contaminant, 3) a volumetrically significant degree of contamination, and 4) a contaminant that has experienced low-temperature alteration to produce high- $\delta^{18}\text{O}$ . These are equally attributable to the Suldal Arc as they are in the western US examples, thus, a similar geodynamic process is postulated for the Suldal Arc (Figure 9).

Although the exact mechanism that contributed high- $\delta^{18}\text{O}$  material to the magma generation of the Suldal Arc cannot be uniquely determined from the available data, a model that is compatible with the data is that of accretion of young and juvenile material (i.e. oceanic crust) with overlying sediments of mixed age, to the pre-existing continental margin, underthrusting of this material to a deep-crustal/upper-mantle location, and mobilization via arc magmatism generated in a deep-crustal melting zone (Figure 9). From the current knowledge of the region and available data, it is unknown how much of the Hardangervidda-Rogaland Block comprised pre-existing continental substrate, or how much originated as accreted juvenile material; however, following the arguments outlined above for deep-crustal mixing, i.e. no zircon inheritance, no exotic xenoliths, and no exposed older crust, it is argued that any pre-existing felsic substrate was volumetrically minor within the exposed region of the Suldal Arc.

### **Continental growth**

The comparison between the Suldal Arc with batholiths of the western US cordilleran system is pertinent, because the latter provides an example of the dominant continental crust formation process that exists in the Phanerozoic (Lee et al., 2007); thus, crustal formation processes in the Proterozoic can be compared to those in the Phanerozoic, with implications for the uniformitarianism of plate tectonics through time, a theme that is still widely debated

(e.g. Ernst, 2009; Hamilton, 2010; Shirey & Richardson, 2011). In the Phanerozoic example, building of the Sierra Nevada and Peninsular Range batholiths produced crust that is similar in composition to the average upper continental crust (Lee et al., 2007); the differentiation from basaltic parent magmas to felsic upper crust was aided by delamination of gabbroic and garnet pyroxenite cumulates and restites (Lee et al., 2006; 2007). Figure 10 shows a comparison between the average concentration of major and trace elements of the Suldal Arc compared to an average upper continental crust composition (UCC; Rudnick & Gao, 2003). The average Suldal Arc may be biased by sampling, since no correction for outcrop area, or estimated volume is taken into account; however, the 65% SiO<sub>2</sub> of this average suggests it may be a suitable representation of the upper crust, given its similarity to the 66% of the average upper continental crust model. The multi-element pattern is remarkably similar, the only significant difference being that the Suldal Arc has elevated concentrations of middle to heavy REEs compared to UCC. This could be reconciled if the percentage of mafic to felsic compositions was under-represented in the sample set; however, from observations in the field this isn't expected to be the case at the exposed crustal level. An alternative is that minerals that preferentially remove middle to heavy REE's from evolving melts may have had less involvement in the Suldal Arc; for example, a thinner crustal pile would involve less garnet. Without data from lower crustal lithologies, this avenue is not explored; however, the similarity between the chemistry and isotope systematics of the western US batholiths and the Suldal Arc, and the ability to fit a comparable petrotectonic model between the two examples, suggests processes such as cumulate delamination are likely to have been involved in the older as well as the younger example.

An additional process that helps drive magmatic compositions from parental mantle-like melts to that of the average continental crust, is the addition of sedimentary material to arc

magmas; for example, in the Honshu arc system, mixing between partial melts of arc basalt with 30% melt contribution of metasediments, produces compositions of the Kaikomagatake pluton that are comparable to the average UCC (Saito et al., 2011). These metasediments are derived from the collisional nature of the arc, whereby the oceanic Izu-Bonin arc is colliding with the mature Honshu arc; thus, this setting is rather analogous to the western US batholiths, whereby formation of mature continental arc compositions occurs after accretion of juvenile oceanic arcs/terrane to the continental margin. This comparison between all of the examples discussed, suggests that processes such as crustal thickening and tectonic underthrusting may form integral parts in producing continental crust, and that similar crust-forming processes may have been acting for at least the last 1500 Ma.

#### **The origin of the Hardangervidda-Rogaland and Telemark Blocks**

The evolution of the Suldal Arc postulated here (figure 9), represents the central part of the Hardangervidda-Rogaland Block, but is probably also an approximate representation of the origin of the Hardangervidda and Rogaland Vest-Agder regions to the north and south respectively (figure 1), since similar aged gneiss complexes are found in the region (T. Slagstad & M. Marker, unpublished data). Whether the petrogenetic and geodynamic scenario can be extended to the more easterly Telemark Block is currently unresolved, since there is a dearth of data from the older units within this region. Here, some constraints are discussed, but it is noted that these currently remain speculative. Exposed directly to the east of the Suldal Arc in the Telemark Block, the Tuddal Fm. comprises voluminous rhyolitic volcanism that is dated at ~1512 to ~1500 Ma (Dahlgren et al. 1990; Bingen et al., 2005). This volcanism is suggested to have occurred inboard of a convergent margin in a similar scenario to the granite-rhyolite province of the US (Slagstad et al., 2009), which would fit with the model proposed here of east-dipping subduction under the Sauda-Suldal region. The Tuddal

Fm. is hypothesised to have marked the onset of a continental rift- system that developed into an epicontinental sea (Lamminen & Köykkä, 2010); it can be envisaged that in these authors' model, the Tuddal Fm. would have resulted from crustal anatexis as a consequence of rise of asthenospheric mantle to the base of the crust during lithospheric extension. However, the underthrusting of continent-derived material, as envisaged in figure 9, requires a compressional setting. Two scenarios can resolve this issue: 1) the geodynamic regime changed from compressional prior to 1510 Ma, to extensional after this time, or 2) the Tuddall Fm. formed in a compressional setting. The latter could be a viable process if the crustal anatexis that formed the Tuddall Fm. is linked to overthickening of the continental crust, delamination of a lower crustal root, and subsequent uprise of hot mantle; as this would occur in a strongly compressional regime within a subduction environment (e.g. DeCelles et al., 2009). Given that the Tuddall Fm. was followed by voluminous basaltic magmatism and then sedimentation in a deepening basin, an extensional setting must have prevailed soon after 1500 Ma, irrespective of the geodynamic regime prior to this time.

Andersen et al. (2002b; 2009b) advocated older continental crust of 1.7-1.9 Ga age underlying all of SW Fennoscandia, and use this to argue that the blocks (terranes) of southern Norway (i.e. Hardangervidda-Rogaland, Telemark, Bamble-Lillesand, and Kongsberg-Marstrand) have always been part of the Fennoscandian Shield, rather than being exotic additions accreted during the Sveconorwegian orogeny; their data however do not extend as far west as the Suldal Arc studied here. The model presented here does not require older basement underlying the Sauda-Suldal region of the Hardangervidda-Rogaland Block, but does invoke remobilisation of material of this age from the subducting/accreting/underthrusting oceanic lithosphere and overlying sediments. Thus, it seems possible that the Suldal Arc was a juvenile block of crust that formed outboard of other crustal blocks within SW Fennoscandia

that show evidence of an older crustal substrate. An alternative is that the isotopic signatures seen in other crustal blocks, that lead Andersen et al. (2002b; 2009b) to their conclusions about a substantial older crustal substrate, may in fact result from similar processes advocated for the Suldal Arc, i.e. underthrusting of continent-derived sediments into the deep-crustal/mantle melting region. The 1.6-1.55 Ga calc-alkaline granitoids and gneisses of the Bamble-Lillesand and Kongsberg-Marstrand blocks have similar moderately juvenile isotopic signatures (Andersen et al., 2002b; 2004a), and thus seem likely candidates for continental arc rocks formed via processes similar to that of the Suldal Arc. If an accretionary orogen is envisaged for the 1.65-1.45 Ga period in SW Fennoscandia, as has been suggested by Åhäll & Connelly (2008), then one can imagine a collage of various immature volcanic arcs, ribbon continents, and continental arcs; all forming within the vicinity of the SW Fennoscandian margin, all originating as rifted fragments, and all possessing varying volumes of older crustal substrate.

## **Conclusions**

A range of metaplutonic/volcanic lithologies sampled from the Sauda-Suldal region in SW Norway reveal a period of magmatism from 1521 to 1485 Ma; the petrology and geochemistry is typical of arc magmas that have evolved from mafic to felsic compositions through fractionation and arc maturation. Modeling of Hf-O isotopes is compatible with mixing between end-members that include mantle-derived material, young low-temperature altered material (oceanic crust/sediments) and older low-temperature altered material (continent-derived sediments). A lack of xenoliths and xenocrysts (inherited zircons), exposed older crust, AFC trends and S-type geochemistry, and the large degree of crustal/sedimentary material, all point to mixing within a deep-crustal magma-generation zone. A model consistent with all observations comprises accretion of altered oceanic crust and/or overlying

sediments to a pre-existing continental margin, underthrusting to the magma generation zone, and remobilization during arc magmatism that is fluxed by subduction-driven dehydration melting of the mantle wedge. The addition of sedimentary material to arc magmas drives the compositions towards that of continental crust, as does the potential delamination of cumulate material that is likely to occur in this scenario. The geodynamic setting for this arc magmatism is comparable to that seen in more modern continental arcs (e.g. the Sierra Nevada, Peninsular and Coast Range batholiths), with compositions in the Suldal Arc reaching those of average upper continental crust. Underthrusting of sedimentary materials and their subsequent involvement in arc magmatism is perhaps a more widespread mechanism involved in continental growth than is currently recognised, this has been hindered by the fact that whole-rock geochemistry may not readily reveal such processes. The Suldal Arc magmatism represents a significant crustal addition to SW Fennoscandia; however, the data do not constrain whether such growth was occurring during an indigenous or exotic position to Proterozoic Fennoscandia.

## **Acknowledgements**

This research was funded by a NERC studentship (NER/S/A/2006/14155) to NMWR, and grants NIGFSC IP/994/1107 and NERC IMF 354/1008 to RRP. The authors thank Tom Andersen and Ilya Bindeman for constructive comments that improved the manuscript. The Nordsim facility is operated under an agreement between the research funding agencies of Denmark, Norway and Sweden, the Geological Survey of Finland and the Swedish Museum of Natural History. This is NORDSIM contribution number xx.

## **References**

Åhäll, K.-I., Cornell, D.H., Armstrong, R.A., 1998. Ion probe dating of metasedimentary units across the Skagerrak: new constraints for early Mesoproterozoic growth of the Baltic Shield. *Precambrian Research* 87, 117-134.

Åhäll, K.-I., Connelly, J.N., 2008. Long-term convergence along SW Fennoscandia: 330 m.y. of Proterozoic crustal growth. *Precambrian Research* 161, 452-474.

Andersen, T., 1997. Radiogenic isotope systematics of the Herefoss granite, South Norway: an indicator of Sveconorwegian (Grenvillian) crustal evolution in the Baltic Shield. *Chemical Geology* 135, 139-158.

Andersen, T., Andresen, A., Sylvester, A.G., 2001. Nature and distribution of deep crustal reservoirs in the southwestern part of the Baltic Shield: evidence from Nd, Sr and Pb isotope data on late Sveconorwegian granites. *Journal of the Geological Society, London* 158, 253-267.

Andersen, T., Andresen, A., Sylvester, A.G., 2002a. Timing of late- to post-tectonic Sveconorwegian granitic magmatism in South Norway. *NGU Bulletin* 440, 5-18.

Andersen, T., Griffin, W.L., Pearson, N.J., 2002b. Crustal Evolution in the SW part of the Baltic Shield: the Hf Isotope Evidence. *Journal of Petrology* 43, 1725-1747.

Andersen, T., Griffin, W.L., Jackson, S.E., Knudsen, T.-L., Pearson, N.J., 2004a. Mid-Proterozoic magmatic arc evolution at the southwest margin of the Baltic Shield. *Lithos* 73, 289-318.

Andersen, T., Laajoki, K., Saeed, A., 2004b. Age, provenance and tectonostratigraphic status of the Mesoproterozoic Blefjell quartzite, Telemark sector, southern Norway. *Precambrian Research* 135, 217-244.

Andersen, T., Griffin, W.L., 2004. Lu-Hf and U-Pb isotope systematics of zircons from the Storgangen intrusion, Rogaland Intrusive Complex, SW Norway: implications for the

composition and evolution of Precambrian lower crust in the Baltic Shield. *Lithos* 73, 271-288.

Andersen, T., Graham, S., Sylvester, A.G., 2007a. Timing and tectonic significance of Sveconorwegian A-type granitic magmatism in Telemark, southern Norway: New results from laser-ablation ICPMS U-Pb dating of zircon. *NGU Bulletin* 447, 17-31.

Andersen, T., Griffin, W.L., Sylvester, A.G., 2007b. Sveconorwegian crustal underplating in southwestern Fennoscandia: LAM-ICPMS U-Pb and Lu-Hf isotope evidence from granites and gneisses in Telemark, southern Norway. *Lithos* 93, 273-287.

Andersen, T., Andersson, U.B., Graham, S., Åberg, G., Simonsen, S.L., 2009a. Granitic magmatism by melting of juvenile continental crust: New constraints on the source of Palaeoproterozoic granitoids in Fennoscandia from Hf isotopes in zircon. *Journal of the Geological Society* 166, 233-247.

Andersen, T., Graham, S., Sylvester, A.G., 2009b. The geochemistry, Lu-Hf isotope systematics, and petrogenesis of Late Mesoproterozoic A-type granites in southwestern Fennoscandia. *Canadian Mineralogist* 47, 1399-1422.

Annen, C., Blundy, J.D., Sparks, R.S.J., 2006. The Genesis of Intermediate and Silicic Magmas in Deep Crustal Hot Zones. *Journal of Petrology* 47, 505-539.

Appleby, S.K., Graham, C.M., Gillespie, M.R., Hinton, R.W., Oliver, G.J.H., EIMF, 2008. A cryptic record of magma mixing in diorites revealed by high-precision SIMS oxygen isotope analysis of zircons. *Earth and Planetary Science Letters* 269, 105-117.

Appleby, S.K., Gillespie, M.R., Graham, C.M., Hinton, R.W., Oliver, G.J.H., Kelly, N.M., 2009. Do S-type granites commonly sample infracrustal sources? New results from an integrated O, U-Pb and Hf isotope study of zircon. *Contributions to Mineralogy and Petrology*, 1-18.

Armstrong, R.L., 1971. Isotopic and chemical constraints on models of magma genesis in volcanic arcs. *Earth & Planetary Science Letters* 12, 137-142.

Auer, S., Bindeman, I., Wallace, P., Ponomareva, V., Portnyagin, M., 2009. The origin of hydrous, high- $\delta^{18}\text{O}$  voluminous volcanism: diverse oxygen isotope values and high magmatic water contents within the volcanic record of Klyuchevskoy volcano, Kamchatka, Russia. *Contributions to Mineralogy and Petrology* 157, 209-230.

Be'eri-Shlevin, Y., Katzir, Y., Valley, J.W., 2009. Crustal evolution and recycling in a juvenile continent: Oxygen isotope ratio of zircon in the northern Arabian Nubian Shield. *Lithos* 107, 169-184.

Bickford, M.E., Mueller, P.A., Kamenov, G.D., Hill, B.M., 2008. Crustal evolution of southern Laurentia during the Paleoproterozoic: Insights from zircon Hf isotopic studies of ca. 1.75 Ga rocks in central Colorado. *Geology* 36, 555-558.

Bindeman, I.N., Ponomareva, V.V., Bailey, J.C., Valley, J.W., 2004. Volcanic arc of Kamchatka: A province with high- $\delta^{18}\text{O}$  magma sources and large-scale  $^{18}\text{O}/^{16}\text{O}$  depletion of the upper crust. *Geochimica et Cosmochimica Acta* 68, 841-865.

Bingen, B., Van Breemen, O., 1998. Tectonic regimes and terrane boundaries in the high-grade Sveconorwegian belt of SW Norway, inferred from U-Pb zircon geochronology and geochemical signature of augen gneiss suites. *Journal of the Geological Society, London* 155, 143-154.

Bingen, B., Birkeland, A., Nordgulen, Ø., Sigmond, E.M.O., 2001. Correlation of supracrustal sequences and origin of terranes in the Sveconorwegian orogen of SW Scandinavia: SIMS data on zircon in clastic metasediments. *Precambrian Research* 108, 293-318.

- Bingen, B., Mansfeld, J., Sigmond, E.M.O., Stein, H.J., 2002. Baltica-Laurentia link during the Mesoproterozoic: 1.27 Ga development of continental basins in the Sveconorwegian Orogen, southern Norway. *Canadian Journal of Earth Sciences* 39, 1425-1440.
- Bingen, B., Nordgulen, Ø., Sigmond, E.M.O., Tucker, R., Mansfeld, J., Högdahl, K., 2003. Relations between 1.19-1.13 Ga continental magmatism, sedimentation and metamorphism, Sveconorwegian province, S Norway. *Precambrian Research* 124, 215-241.
- Bingen, B., Skår, Ø., Marker, M., Sigmond, E.M.O., Nordgulen, Ø., Ragnhildstveit, J., Mansfeld, J., Tucker, R.D., Liégeois, J.-P., 2005. Timing of continental building in the Sveconorwegian orogen, SW Scandinavia. *Norsk Geologisk Tidsskrift* 85, 87-105.
- Bingen, B., Andersson, J., Söderlund, U., Möller, C., 2008a. The Mesoproterozoic in the Nordic countries. *Episodes* 31, 29-34.
- Bingen, B., Davis, W.J., Hamilton, M.A., Engvik, A.K., Stein, H.J., Skår, Ø., Nordgulen, Ø., 2008b. Geochronology of high-grade metamorphism in the Sveconorwegian belt, S. Norway: U-Pb, Th-Pb and Re-Os data. *Norsk Geologisk Tidsskrift* 88, 13-42.
- Bolhar, R., Weaver, S.D., Whitehouse, M.J., Palin, J.M., Woodhead, J.D., Cole, J.W., 2006. Sources and evolution of arc magmas inferred from coupled O and Hf isotope systematics of plutonic zircons from the Cretaceous Separation Point Suite (New Zealand). *Earth and Planetary Science Letters* 268, 312-324.
- Brewer, T.S., Daly, J.S., Åhäll, K.-I., 1998. Contrasting magmatic arcs in the Palaeoproterozoic of the south-western Baltic Shield. *Precambrian Research* 92, 297-315.
- Brewer, T.S., Åhäll, K.-I., Menuge, J.F., Storey, C.D., Parrish, R.R., 2004. Mesoproterozoic bimodal volcanism in SW Norway, evidence for recurring pr-Sveconorwegian continental margin tectonism. *Precambrian Research* 134, 249-273.

- Brophy, J.G., 2008. A study of rare earth element (REE)-SiO<sub>2</sub> variations in felsic liquids generated by basalt fractionation and amphibolite melting: A potential test for discriminating between the two different processes. *Contributions to Mineralogy and Petrology* 156, 337-357.
- Cawood, P.A., Kröner, A., Collins, W.J., Kusky, T.M., Mooney, W.D., Windley, B.F., 2009. Accretionary orogens through Earth history. In: Cawood, P.A. & Kröner, A. (eds.) *Earth Accretionary Systems in Space and Time*, Geological Society of London, Special Publication 318, 1-36.
- Chappell, B.W., White, A.J.R., 1974. Two contrasting granite types. *Pacific Geology* 8, 173-174.
- Chauvel, C., Marini, J.-C., Plank, T., Ludden, J.N., 2009. Hf-Nd input flux in the Izu-Mariana subduction zone and recycling of subducted material in the mantle. *Geochemistry, Geophysics, Geosystems* 10, Q01001, doi:10.1029/2008GC002101.
- Corfu, F., Hanchar, J.M., Hoskin, P.W.O., Kinny, P., 2003. Atlas of Zircon Textures. *Reviews in Mineralogy and Geochemistry* 53, 469-500.
- Dahlgren, S., Heaman, L., Krogh, T., 1990. Geological evolution and U-Pb geochronology of the Proterozoic central Telemark area, Norway. *Geonytt* 17, 38-39.
- Davidson, J., 1985. Mechanisms of contamination in Lesser Antilles island arc magmas from radiogenic and oxygen isotope relationships. *Earth and Planetary Science Letters* 72, 163-174.
- de Haas, G.J.L.M., Andersen, T., Vestin, J., 1999. Detrital zircon geochronology: new evidence for an old model for accretion of the SW Baltic Shield. *Journal of Geology* 107, 569-586.
- DeCelles, P.G., Ducea, M.H., Kapp, P., Zandt, G., 2009. Cyclicity in Cordilleran orogenic systems. *Nature Geoscience* 2, 251-257.

Eiler, J.M., Carr, M.J., Reagan, M., Stolper, E., 2005. Oxygen isotope constraints on the sources of Central American arc lavas. *Geochemistry, Geophysics, Geosystems* 6, Q07007, doi:10.1029/2004GC000804.

Ernst, W.G., 2009. Archean plate tectonics, rise of Proterozoic supercontinentality and onset of regional, episodic stagnant-lid behavior. *Gondwana Research* 15, 243-253.

Frost, B.R., Barnes, C.G., Collins, W.J., Arculus, R.J., Ellis, D.J., Frost, C.D., 2001. A Geochemical Classification for Granitic Rocks. *Journal of Petrology* 42, 2033-2048.

Gaál, G., Gorbatschev, R., 1987. An Outline of the Precambrian evolution of the Baltic Shield. *Precambrian Research* 35, 15-52.

Gasparon, M., Hilton, D.R., Varne, R., 1994. Crustal contamination processes traced by helium isotopes: Examples from the Sunda arc, Indonesia. *Earth and Planetary Science Letters* 126, 15-22.

Gill, J.B., 1981. *Orogenic Andesites and Plate Tectonics*. Springer-Verlag, New York, 1-390.

Griffin, W.L., Pearson, N.J., Belousova, E., Jackson, S.E., van Achterbergh, E., O'Reilly, S.Y., Shee, S.R., 2000. The Hf isotope composition of cratonic mantle: LAM-MC-ICPMS analysis of zircon megacrysts in kimberlites. *Geochimica et Cosmochimica Acta* 64, 133-147.

Hacker, B.R., Kelemen, P.B., Behn, M.D., 2011. Differentiation of the continental crust by relamination. *Earth and Planetary Science Letters* 307, 501-516.

Hamilton, W.B., 2010. Plate tectonics began in Neoproterozoic time, and plumes from deep mantle have never operated. *Lithos* 123, 1-20.

Hawkesworth, C.J., O'Nions, R.K., Arculus, R.J., 1979. Nd and Sr isotope geochemistry of island arc volcanics, Grenada, Lesser Antilles. *Earth and Planetary Science Letters* 45, 237-248.

Hildreth, W., Moorbath, S., 1988. Crustal contributions to arc magmatism in the Andes of Central Chile. *Contributions to Mineralogy and Petrology* 98, 455-489.

Högdahl, K., Andersson, U.B., Eklund, O., 2004. The transscandinavian Igneous Belt (TIB) in Sweden: A review of its character and evolution. *Special Paper of the Geological Survey of Finland* 37, 1-125.

James, D.E., 1981. The combined use of oxygen and radiogenic isotopes as indicators of crustal contamination. *Annual Reviews in Earth and Planetary Science* 15, 395-396.

Johnson, E.R., Wallace, P.J., Granados, H.D., Manea, V.C., Kent, A.J.K., Bindeman, I.N., Donegan, C.S., 2009. Subduction-related Volatile Recycling and Magma Generation beneath Central Mexico: Insights from Melt Inclusions, Oxygen Isotopes and Geodynamic Models. *Journal of Petrology* 50, 1729-1764.

Kemp, A.I.S., Hawkesworth, C.J., Foster, G.L., Paterson, B.A., Woodhead, J.D., Hergt, J.M., Gray, C.M., Whitehouse, M.J., 2007. Magmatic and crustal differentiation history of granitic rocks from Hf-O isotopes in zircon. *Science* 315, 980-983.

Kemp, A.I.S., Hawkesworth, C.J., Collins, W.J., Gray, C.M., Blevin, P.L., 2009. Isotopic evidence for rapid continental growth in an extensional accretionary orogen: The Tasmanides, eastern Australia. *Earth and Planetary Science Letters* 284, 455-466.

Korja, A., Lahtinen, R., Nironen, M., 2006. The Svecofennian orogen: a collage of microcontinents and island arcs. In: Gee, D.G. and Stephenson, R.A. (Eds.), *European Lithosphere Dynamics*. Geological Society of London Memoirs 32, 561-578.

Laajoki, K., Corfu, F., Andersen, T., 2002. Lithostratigraphy and U-Pb geochronology of the Telemark supracrustals in the Bandal-Sauland area, Telemark, South Norway. *Norwegian Journal of Geology* 82, 119-138.

Lackey, J.S., Valley, J.W., Saleeby, J.B., 2005. Supracrustal input to magmas in the deep crust of Sierra Nevada batholith: Evidence from high- $\delta^{18}\text{O}$  zircon. *Earth and Planetary Science Letters* 235, 315-330.

Lahtinen, R., Korja, A., Nironen, M., Heikkinen, P., 2009. Palaeoproterozoic accretionary processes in Fennoscandia. In: Cawood, P.A. & Kröner, A. (eds.) *Earth Accretionary Systems in Space and Time*, Geological Society of London, Special Publication 318, 237-256.

Lamminen, J., Köykkä, J., 2010. The provenance and evolution of the Rjukan Rift Basin, Telemark, south Norway: The shift from a rift basin to an epicontinental sea along a Mesoproterozoic supercontinent. *Precambrian Research* 181, 129-149.

Lee, C.-T.A., Cheng, X., Horodyskyj, U., 2006. The development and refinement of continental arcs by primary basaltic magmatism, garnet pyroxenite accumulation, basaltic recharge and delamination: insights from the Sierra Nevada, California. *Contributions to Mineralogy and Petrology* 151, 222-242.

Lee, C.-T.A., Mortin, D.M., Kistler, R.W., Baird, A.K., 2007. Petrology and tectonics of Phanerozoic continent formation: From island arcs to accretion and continental arc magmatism. *Earth and Planetary Science Letters* 263, 370-387.

Martin, E., Bindeman, I., Grove, T.L., 2011. The origin of high-Mg magmas in Mt Shasta and Medicine Lake volcanoes, Cascade Arc (California): higher and lower than mantle oxygen isotope signatures attributed to current and past subduction. *Contributions to Mineralogy and Petrology* 162, 945-960.

Miller, C.F., McDowell, S.M., Mapes, R.W., 2003. Hot and cold granites: Implications of zircon saturation temperatures and preservation of inheritance. *Geology* 31, 529-532.

Nebel, O., Vroon, P.J., van Westrenen, W., Iizuka, T., Davies, G. R., 2011. The effect of sediment recycling in subduction zones on the Hf isotope character of new arc crust, Banda arc, Indonesia. *Earth and Planetary Science Letters* 303, 240-250.

Pearce, J.A., 1983. Role of the sub-continental lithosphere in magma genesis at active continental margins. In: Hawesworth, C.J. & Norry, M.J. (eds.) *Continental Basalts and Mantle Xenoliths*, Cheshire, U.K., Shiva Publishing Limited, 230-249.

Peck, W.H., Valley, J.W., Corriveau, L., Davidson, A., McLelland, J., Farber, D.A., 2004. Oxygen-isotope constraints on terrane boundaries and origin of 1.18-1.13 Ga granitoids in the southern Grenville Province. In: Tollo, R.P., Corriveau, L., McLelland, J. and Bartholomew, M.J.I. (Eds.), *Proterozoic Tectonic Evolution of the Grenville Orogen in North America*. Geological Society of America Memoir 197, 163-182.

Pedersen, S., Andersen, T., Konnerup-Madsen, J., Griffin, W.L., 2009. Recurrent Mesoproterozoic continental magmatism in South-Central Norway. *International Journal of Earth Science* 98, 1151-1171.

Plank, T., Langmuir, C.H., 1993. Tracing trace elements from sediment input to volcanic output at subduction zones. *Nature* 362, 739-743.

Portnyagin, M., Hoernle, K., Plechov, P., Mironov, N., Khubunaya, S., 2007. Constraints on mantle melting and composition and nature of slab components in volcanic arcs from volatiles (H<sub>2</sub>O, S, Cl, F) and trace elements in melt inclusions from the Kamchatka Arc. *Earth and Planetary Science Letters* 255, 53-69.

Roberts, N.M.W., Parrish, R.R., Horstwood, M.S.A., Brewer, T., 2011. The 1.23 Ga Fjellhovdane rhyolite, Grøssæ-Totak; a new age within the Telemark supracrustals, southern Norway. *Norwegian Journal of Geology* 91, 239-246.

Rudnick, R.L., Gao, S., 2003. Composition of the continental crust. *Treatise on Geochemistry* 3, 1-64.

Salters, V.J.M., Stracke, A., 2004. Composition of the depleted mantle. *Geochemistry Geophysics Geosystems* 5, Q05B07, doi:10.1029/2003GC000597.

Saito, S., Arima, M., Nakajima, T., Tani, K., Miyazaki, T., Senda, R., Chang, Q., Takahashi, T., Hirahara, Y., Kimura, J.-I., 2012. Petrogenesis of the Kaikomagatake granitoids pluton in the Izu Collision Zone, central Japan: implications for transformation of juvenile oceanic arc into mature continental crust. *Contributions to Mineralogy and Petrology* 163, 611-629.

Schärer, U., Wilmart, E., Duchesne, J.-C., 1996. The short duration and anorogenic character of anorthosite magmatism: U-Pb dating of the Rogaland complex, Norway. *Earth and Planetary Science Letters* 139, 335-350.

Shirey, S.B., Richardson, S.H., 2011. Start of the Wilson Cycle at 3 Ga Shown by Diamonds from Subcontinental Mantle. *Science* 333, 434-436

Simon, L., Lécuyer, C., 2005. Continental recycling: The oxygen isotope point of view. *Geochemistry Geophysics Geosystems* 6, Q08004, doi:10.1029/2005GC000958.

Sigmond, E.M.O., 1975. Geologisk kart over Norge, berggrunnskart Sauda, 1:250000. Geological Survey of Norway.

Sigmond, E.M.O., 1978. Beskrivelse til det berggrunnsgeologiske kartbladet Sauda 1:250000. NGU Bulletin 341, 1-94.

Sigmond, E.M.O., 1985. The Mandal-Ustaoset line, a newly discovered major fault zone in south Norway. In: Tobi, A. C., Touret, J. L., (Eds.), *The Deep Proterozoic Crust in the North Atlantic Provinces*. NATO ASI Series. Reidel, Dordrecht, 323-331.

Slagstad, T., Culshaw, N.G., Daly, J.S., Jamieson, R.A., 2009. Western Grenville Province holds key to midcontinental Granite-Rhyolite Province enigma. *Terra Nova* 21, 181-187.

Slagstad, T., Roberts, N.M.W., Marker, M., Røhr, T., Schiellerup, H., 2012. A non-collisional, accretionary Sveconorwegian orogen. *Terra Nova*, doi: 10.1111/ter.12001.

Sun, S.S., McDonough, 1989. Chemical and isotopic systematics of oceanic basalts: implications for mantle composition and processes. In: Saunders, A.D. and Norry, M.J. (Eds.), *Magmatism in the Ocean Basins*. Geological Society of London, Special Publication 42, 313-345.

Thirlwall, M.F., Graham, A.M., 1984. Evolution of high-Ca, high-Sr C-series basalts from Grenada, Lesser Antilles: the effects of intra-crustal contamination. *Journal of the Geological Society* 141, 427-445.

Tollstrup, D., Gill, J., Kent, A., Prinkey, D., Williams, R., Tamura, Y., Ishizuka, O., 2010. Across-arc geochemical trends in the Izu-Bonin arc: Contributions from the subducting slab, revisited. *Geochemistry, Geophysics, Geosystems* 11, Q01X10, doi:10.1029/2009GC002847.

Valley, J.W., Kinny, P.D., Schulze, D.J., Spicuzza, M.J., 1998. Zircon megacrysts from kimberlite: Oxygen isotope variability among mantle melts. *Contributions to Mineralogy and Petrology* 133, 1-11.

Valley, J.W., Lackey, J.S., Cavosie, A.J., Clechenko, C.C., Spicuzza, M.J., Basei, M.A.S., Bindeman, I.N., Ferreira, V.P., Sial, A.N., King, E.M., Peck, W.H., Sinha, A.K., Wei, C.S., 2005. 4.4 billion years of crustal maturation: Oxygen isotope ratios of magmatic zircon. *Contributions to Mineralogy and Petrology* 150, 561-580.

Vander Auwera, J., Bolle, O., Bingen, B., Liégeois, J.-P., Bogaerts, M., Duchesne, J.C., De Waele, B., Longhi, J., 2011. Sveconorwegian massif-type anorthosites and related granitoids

result from post-collisional melting of a continental arc root. *Earth-Science Reviews* 107, 375-397.

Vroon, P.Z., Lowry, D., Van Bergen, M.J., Boyce, A.J., Matthey, D.P., 2001. Oxygen isotope systematics of the Banda Arc: Low  $\delta^{18}\text{O}$  despite involvement of subducted continental material in magma genesis. *Geochimica et Cosmochimica Acta* 65, 589-609.

Watson, E.B., Harrison, T.M., 1983. Zircon saturation revisited: temperature and composition effects in a variety of crustal magma types. *Earth and Planetary Science Letters* 64, 295-304.

Watson, E.B., 1996. Dissolution, growth and survival of zircons during crustal fusion: Kinetic principles, geological models and implications for isotopic inheritance. *Transactions of the Royal Society of Edinburgh, Earth Sciences* 87, 43-56.

Wetmore, P.H., Ducea, M.N., 2011. Geochemical evidence of a near-surface history for source rocks of the central Coast Mountains Batholith, British Columbia. *International Geology Review* 53, 230-260.

## **Figures**

Figure 1. Geological map of the Suldal Sector, based on Sigmond (1975), and with additional unpublished mapping by the Geological Survey of Norway (T. Slagstad & M. Marker, unpublished data). Inset shows Proterozoic crustal blocks within southwest Fennoscandia. New U-Pb ages presented here are shown with the corresponding sample locations.

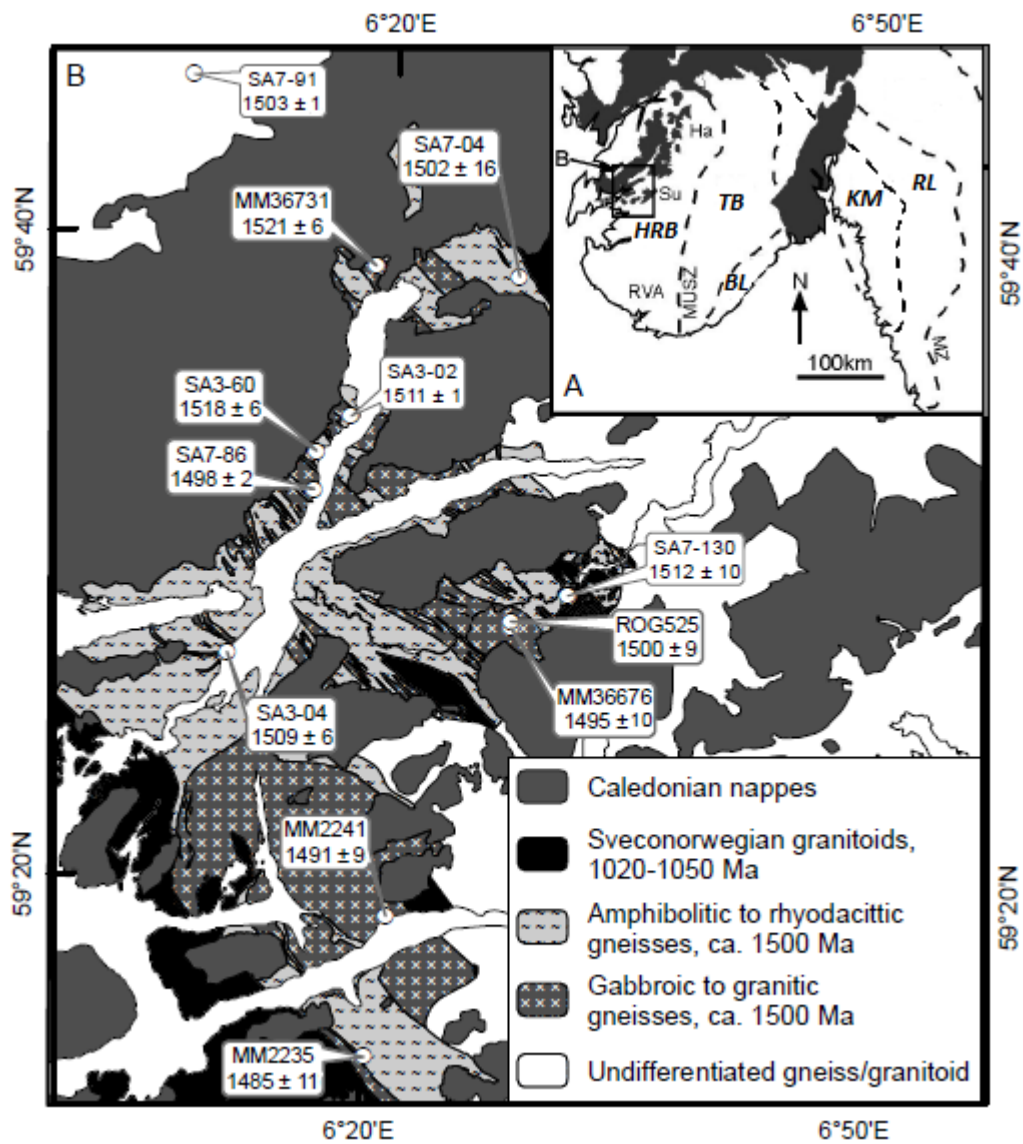


Figure 2. A) Compilation of U-Pb ages from the Suldal Sector for Telemarkian (1520-1480 Ma) magmatism. B) All in-situ U-Pb data for Telemarkian magmatism in the Suldal Sector plotted as a probability density plot; note the lack of >1550 Ma ages.

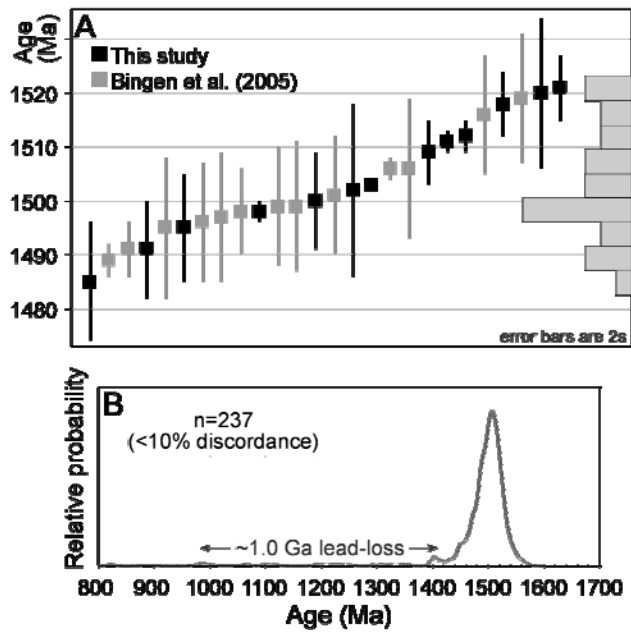


Figure 3. Whole-rock geochemistry of Sauda Grey Gneiss Association and the associated granitoids from the Suldal Sector.  $Fe^*$  = Fe-number ( $FeOt / (FeOt + Mg)$ ), ASI = aluminium saturation index ( $Al / (Ca - 1.67P + Na + K)$ ), MALI = modified alkali-lime index ( $Na_2O + K_2O - CaO$ ) (Frost et al., 2001).

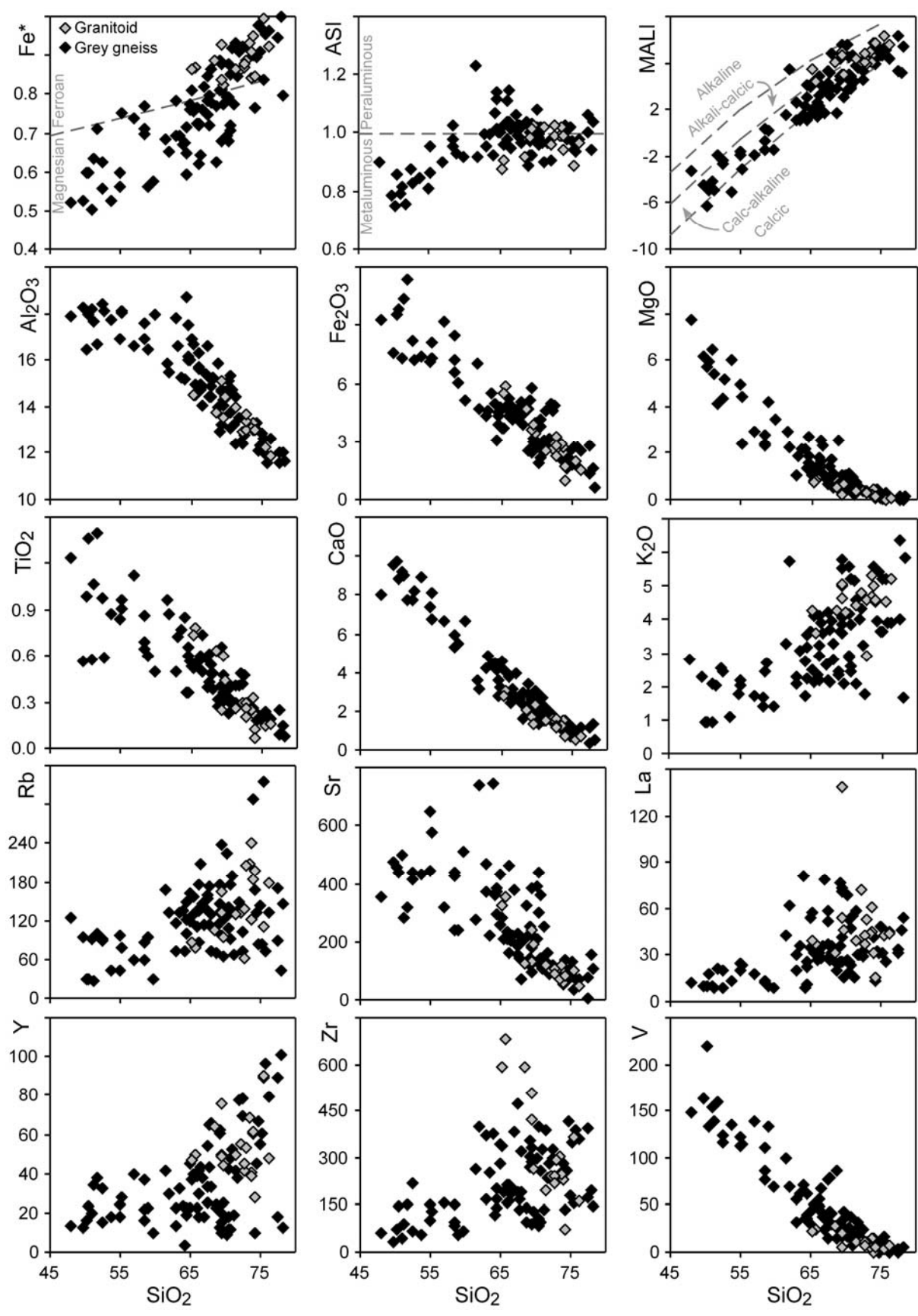


Figure 4. Multi-element primitive-mantle and chondrite-normalised diagrams (using values from Sun & McDonough, 1985), for the SGGA and granitoids from the Suldal Sector.

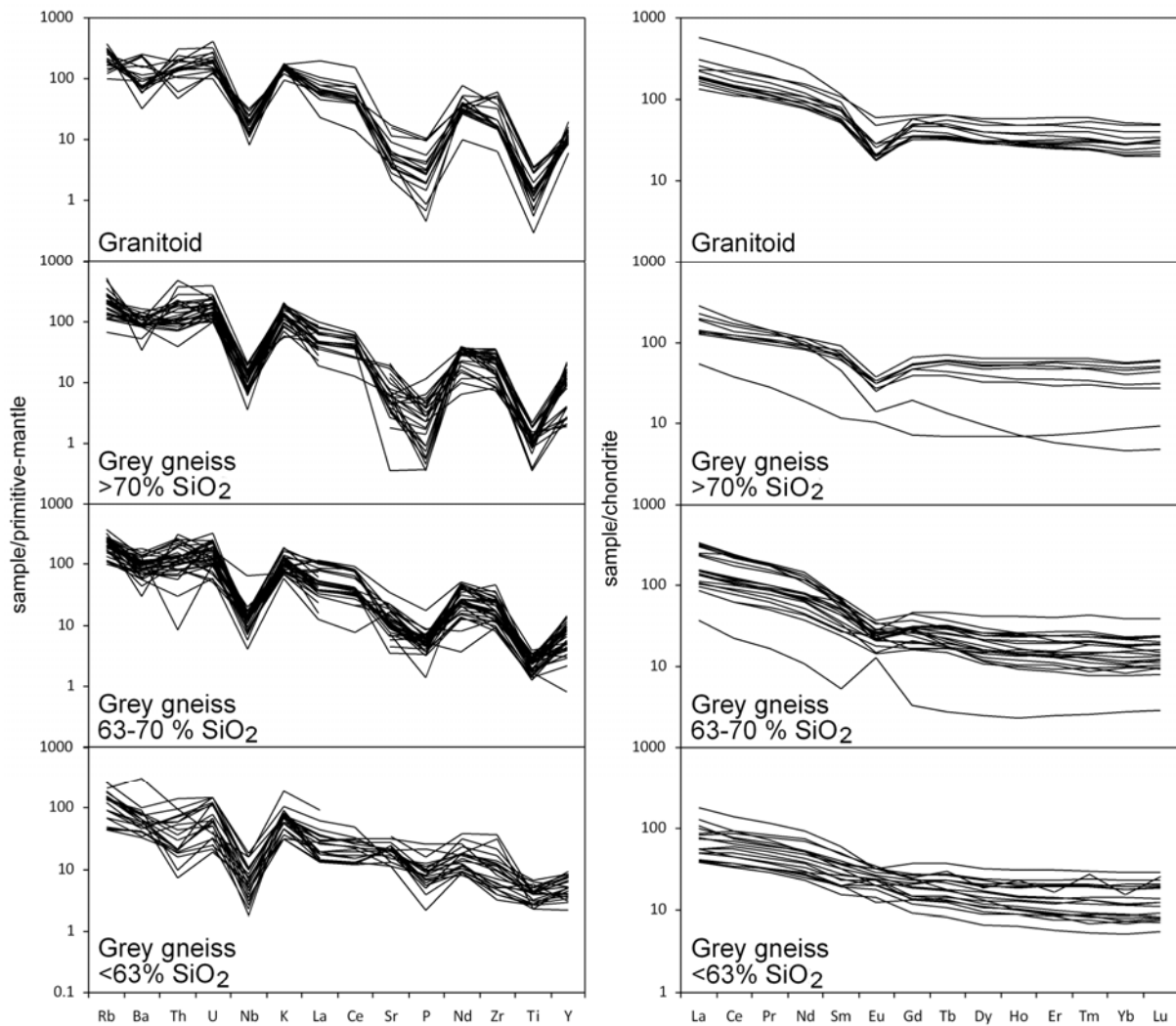


Figure 5. Hf isotope data from the Suldal Sector; A) all data plotted against arbitrary values, B) average values plotted against whole-rock  $\text{SiO}_2$  and U-Pb age.

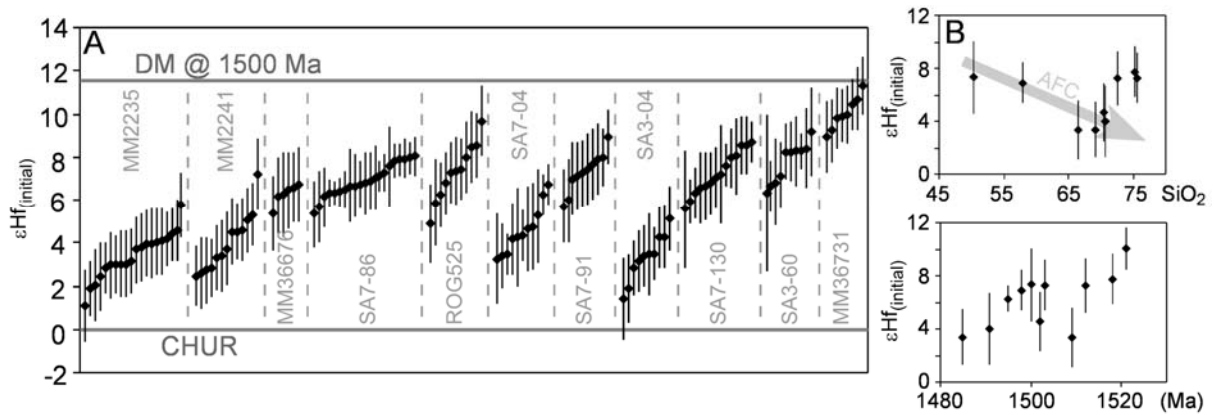


Figure 6. O isotope data from the Suldal Sector; A) all data plotted against arbitrary values, B) all data averaged and recalculated to melt compositions (see text for explanation) and plotted against whole-rock  $\text{SiO}_2$  (Assimilation Fractional Crystallisation (AFC) trend is arbitrary).

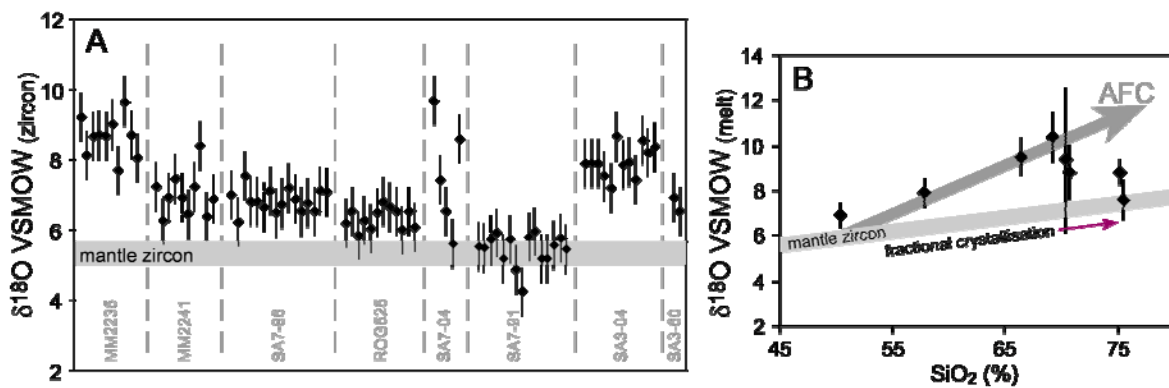


Figure 7. Hf isotope data for SW Fennoscandia plotted against U-Pb crystallisation age, published data from Andersen et al. (2002b; 2004b; 2009a); Depleted Mantle (DM) uses values of Griffin et al. (2000), the evolution of TIB crust uses a 'crustal' Lu/Hf ratio of 0.015; see text for explanation of mantle and crustal end-members.

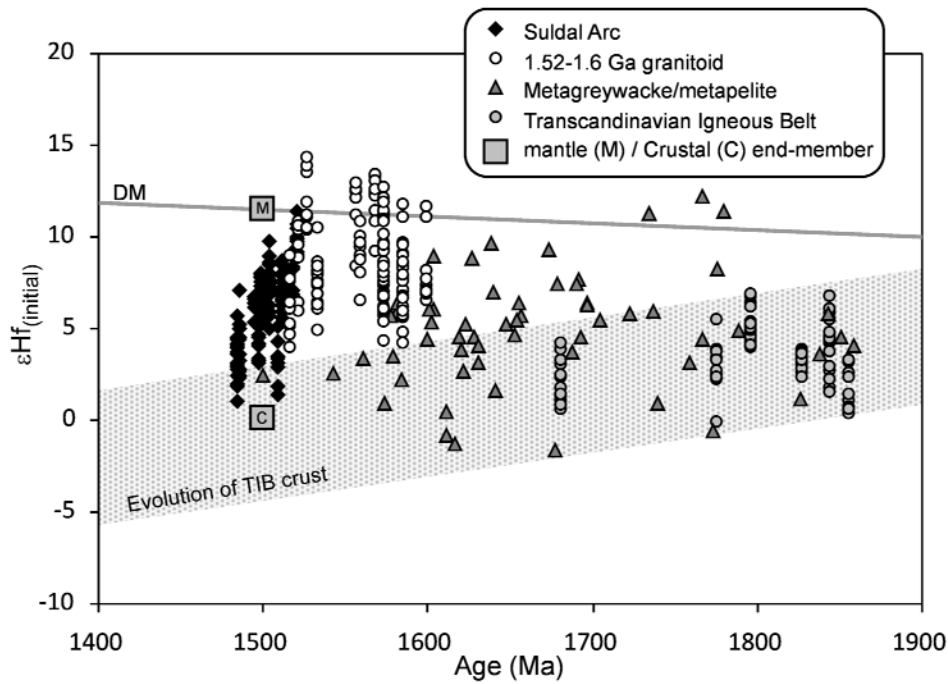


Figure 8. Hf and O isotope data plotted where measured on the same zircon. Depleted Mantle plotted at ~1.5 Ga using values of Griffin et al. (2000); the sedimentary end-members are discussed in the text. The curves in (A) represent mixing between mantle and crustal/sediment end-members using lower-crustal and upper-crustal Hf concentrations for the sediment end-member, and represent source contamination (mantle recycling). The curves in (B) represent two-component mixing between an older sedimentary component, and a younger mixed mantle-crustal component that has mantle-like to moderately elevated  $\delta^{18}\text{O}$ . End-member concentrations based upon Simon & Lécuyer (2005), Salters & Stracke (2004) and Rudnick & Gao (2003).

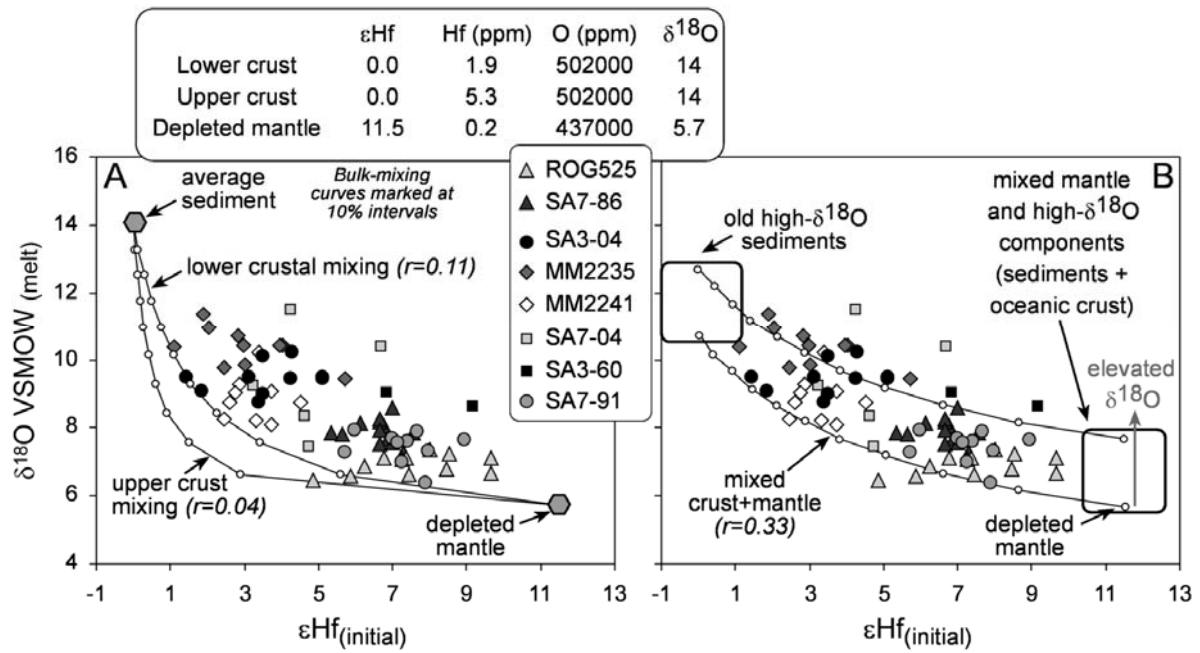


Figure 9. Hypothesised petrotectionic model for formation of the Suldal Arc magmatism, modified from Lackey et al. (2005); 1) Accretion of juvenile lithosphere and sediments to the pre-existing continental margin (this may have comprised oceanic arc material), 2) underplating and underthrusting of altered material to the deep-crust/upper-mantle, 3) subduction mobilizes this high- $\delta$  melting zone, 5) mafic to felsic arc magmas are derived from this deep-crustal magma-generation zone.

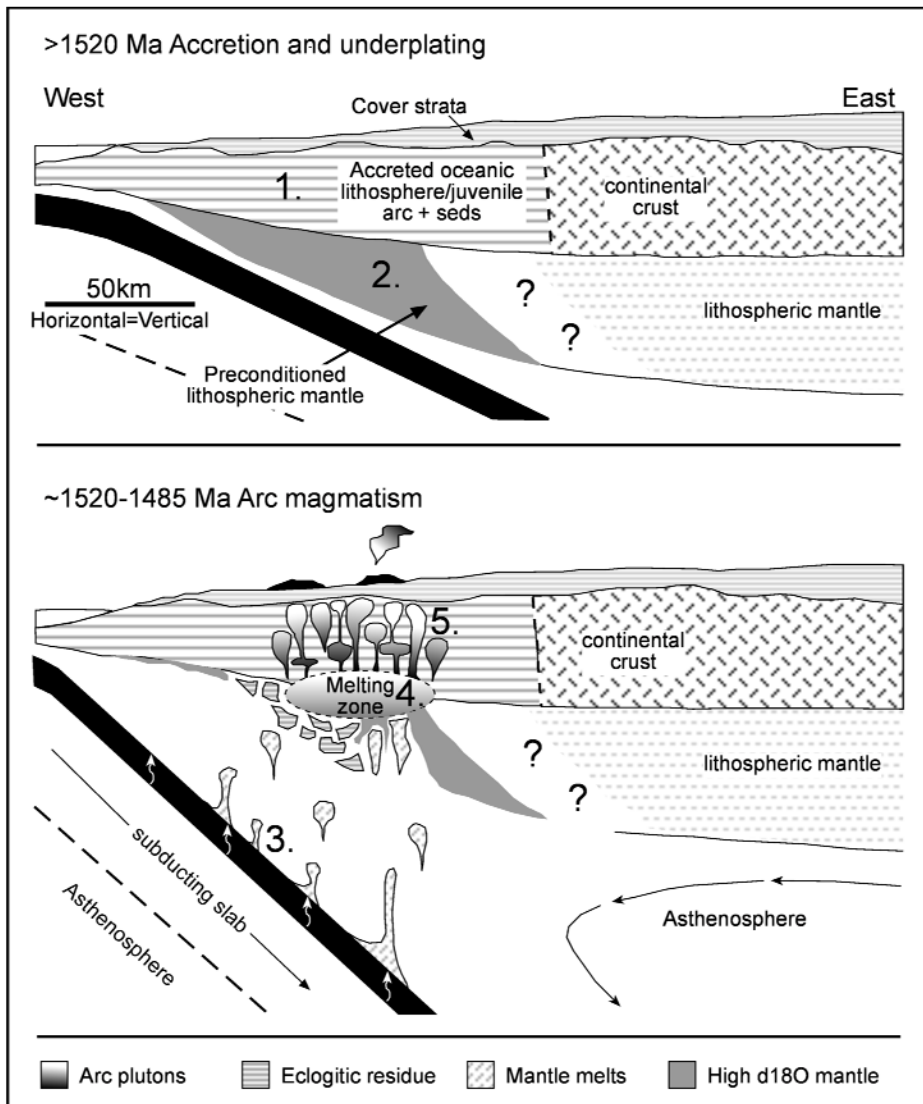


Figure 10. Primitive-mantle normalised multi-element diagram for the average of the Suldal Arc data, compared with the average upper continental crust (UCC) of Rudnick & Gao (2003).

